

Programmable assembly of a metabolic pathway enzyme in a pre-packaged reusable bioMEMS device†

Xiaolong Luo,^{a,f} Angela T. Lewandowski,^{b,d} Hyunmin Yi,^{c,g} Gregory F. Payne,^d Reza Ghodssi,^{e,f} William E. Bentley^{a,d} and Gary W. Rubloff^{*c,f}

Received 7th September 2007, Accepted 14th December 2007

First published as an Advance Article on the web 14th January 2008

DOI: 10.1039/b713756g

We report a biofunctionalization strategy for the assembly of catalytically active enzymes within a completely packaged bioMEMS device, through the programmed generation of electrical signals at spatially and temporally defined sites. The enzyme of a bacterial metabolic pathway, *S*-adenosylhomocysteine nucleosidase (Pfs), is genetically fused with a pentatyrosine “pro-tag” at its C-terminus. Signal responsive assembly is based on covalent conjugation of Pfs to the aminopolysaccharide, chitosan, upon biochemical activation of the pro-tag, followed by electrodeposition of the enzyme–chitosan conjugate onto readily addressable sites in microfluidic channels. Compared to traditional physical entrapment and surface immobilization approaches in microfluidic environments, our signal-guided electrochemical assembly is unique in that the enzymes are assembled under mild aqueous conditions with spatial and temporal programmability and orientational control. Significantly, the chitosan-mediated enzyme assembly can be reversed, making the bioMEMS reusable for repeated assembly and catalytic activity. Additionally, the assembled enzymes retain catalytic activity over multiple days, demonstrating enhanced enzyme stability. We envision that this assembly strategy can be applied to rebuild metabolic pathways in microfluidic environments for antimicrobial drug discovery.

Introduction

Microelectromechanical systems (MEMS) based on semiconductors convey electrical and optical signals and exhibit high throughput analysis. Biological components, such as nucleic acid, enzymes and antibodies, exhibit molecular recognition capabilities for biosensing functions. The integration of biology with MEMS (bioMEMS), especially with microfluidic systems, offers major advances in our ability to manipulate biomolecular systems.^{1–10} The microfluidic environment of bioMEMS devices provides unprecedented advantages for enzyme analysis because of the ability to work with smaller

reagent volumes, shorter reaction times, and the possibility of parallel operation.^{1,2,11,12} Recently, researchers have explored enzyme assembly approaches in microfabricated devices using either entrapment approaches, such as packed beads^{11,13–15} or surface immobilization approaches.^{11,16–25} However, robust and reproducible enzyme assembly within microfluidic devices remains challenging due to the labile nature of these biological molecules that is incompatible with lengthy and dry processing conditions often occurring in the device fabrication.

Additionally, semiconductor-based devices are expensive due to the need of costly photolithographic equipments and the access of clean rooms, and the microfabrication processes are time-consuming. Therefore, tremendous research has been directed to fabricate cheap disposable devices for biological applications by using alternative polymeric materials, such as polydimethylsiloxane (PDMS),^{26–30} and soft lithographic techniques, including microcontact printing.^{19,26–28,31} However, this substitution of polymers for semiconductors as the basis for bioMEMS poses new challenges in (a) integrating multiple electrical and optical functions together with microfluidics, and (b) simultaneously facilitating the incorporation of biological species in the bioMEMS.

In this paper, we report a chitosan-mediated biofunctionalization strategy for the assembly of catalytically active enzymes onto spatially and temporally programmed sites within completely packaged and systematically controlled bioMEMS devices. Specifically, we report assembly of a bacterial metabolic pathway enzyme, *S*-adenosylhomocysteine nucleosidase (Pfs), and demonstrate that it retains catalytic activity for small

^aFischell Department of Bioengineering, University of Maryland, College Park, MD, 20742, USA

^bDepartment of Chemical and Biomolecular Engineering, University of Maryland, College Park, MD, 20742, USA

^cDepartment of Materials Science and Engineering, University of Maryland, College Park, MD, 20742, USA. E-mail: rubloff@umd.edu; Fax: +1 301 314-9920; Tel: +1 301 405-2949

^dUniversity of Maryland Biotechnology Institute (UMBI), University of Maryland, College Park, MD, 20742, USA

^eDepartment of Electrical and Computer Engineering, University of Maryland, College Park, MD, 20742, USA

^fInstitute for Systems Research (ISR), University of Maryland, College Park, MD, 20742, USA

^gDepartment of Chemical and Biological Engineering, Tufts University, Medford, MA, 02155, USA

† Electronic supplementary information (ESI) available: Supplementary information on estimation of enzyme specific activity. See DOI: 10.1039/b713756g

molecule biosynthesis. Pfs catalyzes the irreversible cleavage of *S*-adenosylhomocysteine (SAH) into *S*-ribosylhomocysteine (SRH) and adenine,³² and is a member of the autoinducer-2 (AI-2) biosynthesis pathway, a metabolic pathway found in many bacterial species.³³ AI-2 is a small signaling molecule that mediates interspecies bacterial cell–cell communication termed “quorum sensing” (QS), a process in which the entire population coordinates behavior in response to environmental cues. QS is involved in regulating many of the genes associated with bacterial pathogenesis.^{34–39} Inhibition or knock-down of enzymes in this pathway represents new opportunities for antimicrobial drugs that target population phenotype as opposed to essential biological functions.^{40,41} Therefore, the enzyme assembly strategy reported here provides a template toward rebuilding metabolic pathways in microfluidic environments for novel antimicrobial drug discovery.

Different from conventional approaches, which have immobilized enzymes onto packed beads or on entire surfaces of microchannel walls,^{13–25} our biofunctionalization strategy assembles enzymes at a specific address within a microchannel through the programmed generation of electrical signals at spatially and temporally defined sites. First, the bioMEMS device in Fig. 1(a) is prefabricated for multiple uses. Second, Pfs–chitosan conjugate solution is prepared by covalently conjugating Pfs to chitosan in solution upon tyrosinase activation of the pro-tag genetically fused at the enzyme’s C-terminus, as shown in Fig. 1(b). This conjugation step confers the pH-responsive properties of chitosan to the enzyme Pfs for one-step electro-assembly onto the readily addressable sites within the microfluidic channels. Third, the Pfs–chitosan conjugate is electrodeposited onto an assembly site inside a microfluidic channel by applying negatively biased electrical signals, as shown in Fig. 1(c). With biofunctionalization complete, Fig. 1(d) shows that the Pfs-catalyzed enzymatic reaction is performed by

introducing the enzyme substrate SAH into the microchannel, which is then catalytically converted by the assembled Pfs into products SRH and adenine. After the reaction, Fig. 1(e) indicates that a mild acid wash removes the assembled Pfs–chitosan conjugate for reuse of the bioMEMS.

The unique features of this work are that we employ localized electrical signals to guide the assembly of a biocatalytically-active enzyme at a specific electrode address within a completely packaged microfluidic channel. This assembly approach is important because it allows device fabrication to be separated from biofunctionalization and enables the prefabricated bioMEMS to be repeatedly biofunctionalized for multiple uses.

Materials and methods

Materials

S-adenosylhomocysteine (SAH), bovine serum albumin (BSA), chitosan (minimum 85% deacetylated chitin; molecular weight 200 000 g mol⁻¹) from crab shells, imidazole, isopropyl β -D-thiogalactopyranoside (IPTG), nickel sulfate, phosphate buffered saline (PBS) (2.7 mM KCl, 137 mM NaCl, 1.5 mM KH₂PO₄, 8.1 mM Na₂HPO₄, pH 7.5), sodium cyanoborohydride, and tyrosinase from mushroom were purchased from Sigma (St. Louis, MO, USA). Tyrosinase was reported by the manufacturer to have an activity of 1530 Units mg⁻¹ solid. LB (Luria broth) medium was purchased from Becton Dickinson (Cockeysville, MD, USA). Acetonitrile (HPLC grade), ampicillin sodium salt, chloroform, glycerol, sodium phosphate (monobasic), sodium phosphate (dibasic), and water (HPLC grade) were purchased from Fisher Chemical (Fair Lawn, NJ, USA). Hydrochloric acid and sodium chloride were purchased from J. T. Baker (Phillipsburg, NJ, USA). Non-fat dry milk was purchased from BioRad (Hercules, CA, USA). Bleach was

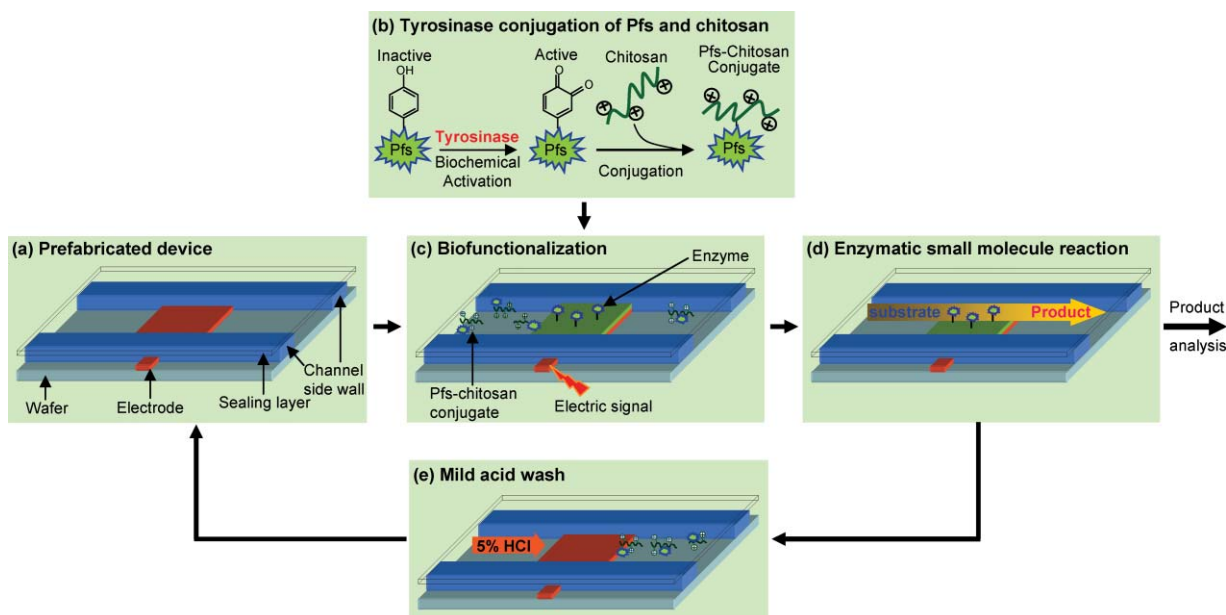


Fig. 1 Schematic flow of programmable enzyme assembly in a pre-packaged reusable bioMEMS device. (a) Prefabricated device, (b) enzyme–chitosan conjugation, (c) electrically programmed assembly of Pfs–chitosan conjugate, (d) enzymatic small-molecule reaction, (e) mild acid wash to remove biofunctionalization and reuse bioMEMS device.

purchased from James Austin Co. (Mars, PA, USA). De-ionized water (ddH_2O , 18 $\text{M}\Omega\text{-cm}$, Milli-Q) and PBS (dissolved in de-ionized water) were autoclaved before use.

Plasmid construction

pTrcHis-Pfs-Tyr plasmid construction was reported elsewhere.⁴² Briefly, the plasmid was constructed by PCR amplification of Pfs from *E. coli* wild type strain W3110. Following digestion, the PCR products were extracted by gel purification and inserted into pTrcHisC (Invitrogen). DNA sequencing was performed to verify construct integrity. The plasmid was transformed into *E. coli* DH5a (defective *luxS* strain).

Purification of $(\text{His})_6\text{-Pfs-(Tyr)}_5$

E. coli DH5a containing pTrcHis-Pfs-Tyr was cultured at 37 °C and 250 rpm in LB medium supplemented with ampicillin at 50 $\mu\text{g mL}^{-1}$. When the $\text{OD}_{600\text{ nm}}$ reached 0.5–0.6, IPTG was added to induce enzyme production at a final concentration of 1 mM IPTG. After an additional 5 h, the culture was centrifuged for 10 min at 10 000 g and the cell pellet stored at –20 °C. The thawed pellet was resuspended in PBS + 10 mM imidazole, pH 7.5, placed in an ice-water bath, and the cells lysed by sonication (Fisher Scientific Sonic Dismembrator 550). The lysed cells were centrifuged for 10 min 16 000 g to remove insoluble cell debris, and the supernatant filtered through 0.22 μm PES filter. The enzyme was purified from the filtered soluble cell extract by immobilized metal-ion affinity chromatography (IMAC) using a 5 mL HisTrap chelating column (Amersham Biosciences). Prior to loading the filtered extract, the column was charged with Ni^{2+} ions using 0.1 M NiSO_4 , washed with de-ionized water, and equilibrated with 3 column volumes (CVs) of

20 mM sodium phosphate, 250 mM NaCl, 10 mM imidazole, pH 7.4. After loading the filtered extract, the column was washed with 3 CVs of the previous buffer, washed again with 3 CVs of 20 mM sodium phosphate, 250 mM NaCl, 50 mM imidazole, pH 7.4, and the protein was eluted using 1.5 CVs of 20 mM sodium phosphate, 250 mM NaCl, 350 mM imidazole, pH 7.4. All steps were performed at 2 mL min^{-1} (1 cm min^{-1} linear velocity). The eluted sample was dialyzed overnight (16 h) at 4 °C into PBS. Purified protein concentration was determined with a UV/vis spectrophotometer (DU 640, Beckman, Fullerton, CA, USA) using UV light at 280 nm wavelength. The protein solution was mixed 2 : 1 with glycerol, aliquoted, and stored at –80 °C.

Chitosan and Pfs–chitosan conjugate preparation

Chitosan solution was prepared by adding chitosan flakes in de-ionized water, with HCl added dropwise to maintain pH \sim 2, and mixing overnight. The pH was then adjusted to pH 4.8 by adding 1 M NaOH dropwise, and the chitosan solution was then filtered and stored at 4 °C.

The conjugate was prepared by incubating $(\text{His})_6\text{-Pfs-(Tyr)}_5$ (0.2 mg mL^{-1}), tyrosinase (0.1 mg mL^{-1} or 166 Units mL^{-1}), and chitosan (0.5% (w/w)) in 50 mM sodium phosphate buffer (final pH of mixture 6.0) for 2 h at room temperature (23–24 °C) and 250 rpm, followed by incubation in sodium cyanoborohydride (0.2 mg mL^{-1}) for 30 min at 250 rpm to stabilize Pfs–chitosan binding.

BioMEMS device fabrication and packaging

The fabrication process of our bioMEMS device with packaging was reported previously.⁴³ Briefly, our bioMEMS device (Fig. 2)

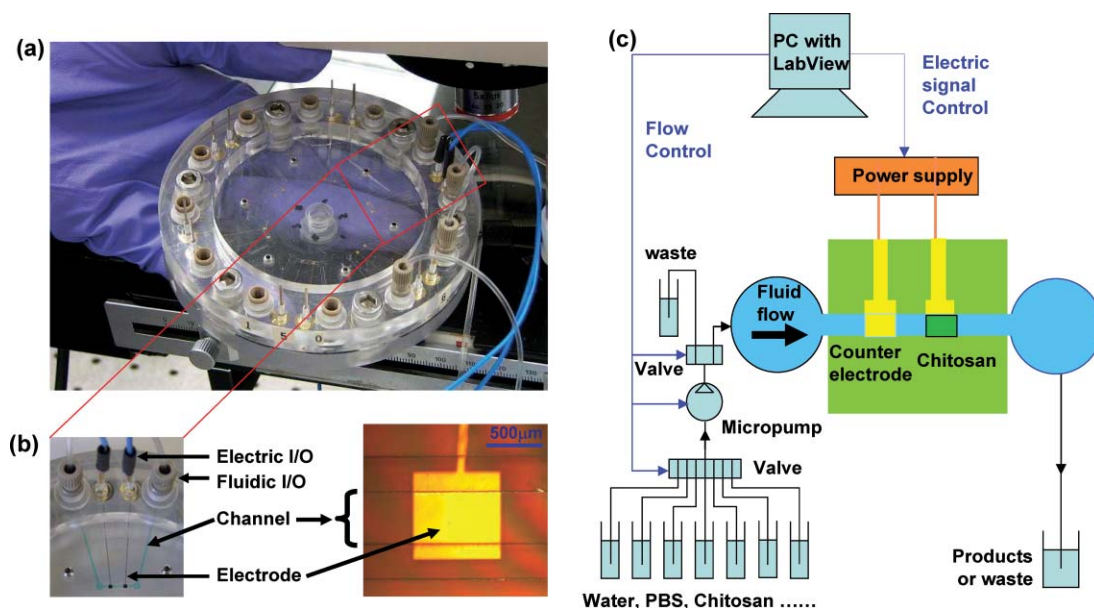


Fig. 2 BioMEMS system and experimental setup. (a) Completely packaged bioMEMS system with electric connectors and fluidic inputs/outputs. There are 6 identical microfluidic channels on a Pyrex wafer which is sealed by a thin PDMS layer and compressed between two Plexiglas plates.⁴³ (b) Colour ink running through one microfluidic channel (left) and zoom-in view of one electrode at the bottom of the channel (right). (c) Schematic bioMEMS control system. A PC with LabView program controls the pumping and selection from different fluids and the chitosan electrodeposition process.

features six identical microchannels evenly distributed on a 4" Pyrex wafer with two rectangular gold electrodes underneath each microchannel. A Cr adhesion layer (90 Å) and then a gold layer (2000 Å) were deposited onto a 4" Pyrex wafer, and rectangular gold electrode patterns (1 mm × 0.5 mm) were created by photolithography. SU8–50 (MicroChem, MA, USA) was patterned on the top of substrate and electrode surfaces to form structures which serve a dual function, namely (1) sidewalls for a microfluidic channel, and (2) sharp “knife-edge” structures for reliable leak-tight sealing to a PDMS layer above. The microfluidic channels were thus sealed by a 300 μm-thick top sealing PDMS layer spun on a Plexiglas plate, and the SU8–50–PDMS junction was compressed by two package-level Plexiglas plates with six pressure-adjustable compression bolts (1/4"-28) hexagonally spaced on the ring and six force tunable socket screws (4–40) between every two microchannels. The microchannels thus formed were 500 μm wide by 150 μm high. Fluidic connectors (Nanoport™) and electric Pogo pins (Interconnect Devices, Inc.) were assembled through punched holes on the sealing PDMS and drilled-holes through the top sealing and packaging Plexiglas plates, and then connected to external pressure-driven aqueous transport and electrical signal, correspondingly.

BioMEMS system control technology

A bioMEMS control system was built to systematically control the selections from multiple solution sources and the pumping into microfluidic channels. The control system shown in Fig. 2 mainly consists of a peristaltic micropump (Masterflex1 pump drive, Cole-Palmer Instrument Co) with two cartridges in alternative directions on an 8-roller cartridge pump head (Masterflex pump head, Cole-Palmer Instrument Co) to achieve near pulseless combined output flow; a 6-to-1 solenoid valve (Bio-Chem Valve/Omnifit, NJ, USA) with separate tubing (0.19 mm ID, Tygon1) to select solutions from multiple sources; a 1-to-2 isolation valve (Bio-Chem Valve/Omnifit, NJ, USA) to direct the pumping either to waste collection or to the bioMEMS

chip; and a LabView-based program which sends digital signals to control solenoid valve selection and to switch the pump on/off, and sends analog signals to control the flow rate. The system is capable of controlling the microfluidic flow rate in a range of 2.8–280 μL min⁻¹. Another LabView program was used to control electrodeposition process and to monitor the voltage of the applied electrical signal (2–3 V measured during the electrodeposition process). A network simulation (VisSim™ 3.2, Design Science Inc.) showed that at 5 μL min⁻¹ flow rate, the velocity inside the channel (cross section: 500 μm × 150 μm) is 1.1 mm s⁻¹. If the pump is restarted after the channel is filled with static fluid, the response time of the flow in the channel is 30 s.

One-step electrodeposition of enzyme–chitosan conjugate and sequential enzymatic reactions

As shown in Table 1, the microchannel and all the connecting tubing were first rinsed with DI water at 50 μL min⁻¹ flow rate for 30 min. Then, bovine serum albumin (BSA) solution (1% (w/v) in PBS buffer) was pumped into the microchannel at 3 μL min⁻¹ for 2 h to block non-specific binding. After PBS buffer rinsing at 3 μL min⁻¹ for 30 min, Pfs–chitosan conjugate solution was pumped into the microchannel at 5 μL min⁻¹. After the microchannel was completely filled, the pump was stopped and an electrical signal of constant current density 3 A m⁻² was applied to maintain negative bias voltage on the gold (working) electrode for 240 s, while a second gold electrode served as the anode (counter). The Pfs–chitosan conjugate solution was then drained from the system, and the electrodeposited Pfs–chitosan conjugate was washed with PBS buffer at 5 μL min⁻¹ and then at 20 μL min⁻¹, each for 15 min. Next, enzymatic reactions were performed by continuously pumping the SAH substrate solution (1 mM SAH in 50 mM sodium phosphate buffer pH 7.2) for 2 h at each flow rate. During the second hour at each flow rate, samples were collected every 10 min for 3 min each. They were then extracted with chloroform and stored at –20 °C before analyzing *via* HPLC.

Table 1 Experimental procedure to demonstrate programmable assembly of a catalytically active enzyme and its reproducibility

	Step #	Procedure	Flow rate/μL min ⁻¹	Time/min
Day 1	1	DI water cleaning	50	
	2	BSA	3	120
	3	PBS buffer	3	30
	4	Pfs–chitosan assembly	Static	4
	5	PBS buffer	5, 20	30
Day 2	6	Enzymatic reaction (SAH)	3, 22	600
	7	HCl wash	22	10
	8	DI water cleaning	50	90
Day 3	9	Enzymatic reaction (SAH)	3	120
	10	DI water cleaning	50	60
	11	BSA	5	120
	12	PBS buffer	5	30
	13	Pfs–chitosan re-assembly	Static	4
	14	PBS buffer	5, 20	30
Day 4	15	Enzymatic reaction (SAH)	3, 22	600
Day 5–7	16	In PBS buffer	Static	3 days
Day 8	17	Enzymatic reaction (SAH)	3, 22	360
	18	Cleaning	50	

Negative controls

Several control experiments were run to evaluate the signal-directed assembly of the conjugate and free enzyme within the MEMS. For control Set #1, the microchannel was incubated for 240 s with free Pfs solution (0.2 mg mL^{-1}) without chitosan (therefore no need of electrical bias) and without tyrosinase. For control Set #2, an electrical signal of constant current density 3 A m^{-2} was first applied for 240 s to electrodeposit chitosan scaffold onto the assembly electrode, then the microchannel was filled with a 5% (w/v) milk–PBS solution to block non-specific binding of Pfs to chitosan and the channel surfaces. Next, a solution of free Pfs solution (0.2 mg mL^{-1}) without tyrosinase was pumped into the microchannel at $5 \mu\text{L min}^{-1}$ for 60 min. For the corresponding experiment, a mixed solution of Pfs (0.2 mg mL^{-1}) and tyrosinase (0.1 mg mL^{-1} or $166 \text{ Units mL}^{-1}$) was pumped into the microchannel at $5 \mu\text{L min}^{-1}$ for 60 min to activate the pro-tag of Pfs *in situ* for its covalent assembly onto the electrodeposited chitosan scaffold. For control Set #3, the process was similar to that shown in Table 1, except there was no electrical signal applied when incubating the microchannel with the same batch of Pfs–chitosan conjugate solution for 240 s. Finally, enzymatic reactions were performed for all sets of controls and the corresponding experiments, and the downstream reaction products were collected and analyzed *via* HPLC.

Analysis of enzymatic reaction products

A Waters Spherisorb Silica column ($250 \times 4.6 \text{ mm}$) with $5 \mu\text{m}$ beads (80 \AA pore) was used in reversed-phase mode with $5 \mu\text{L}$ sample injection size and a mobile phase of 70 : 30 acetonitrile : water at 0.5 mL min^{-1} . Conversion was calculated from elution data at 210 nm . The HPLC system consisted of two Dynamax model SD-200 pumps (with 10 mL pump heads and mixing valve) and a Dynamax Absorbance Detector model UV-D II, and data was analyzed using Star 5.5 Chromatography Software (Rainin).

Results

One-step electrodeposition of enzyme–chitosan conjugate and sequential enzymatic reactions

We demonstrate the assembly of Pfs enzyme onto a readily addressable site in a prefabricated and packaged microfluidic channel by one-step electrodeposition of Pfs–chitosan conjugate. Additionally, we demonstrate retention of catalytic activity of the assembled Pfs, and robustness and stability of the assembled Pfs throughout repeated flow cycles over extended time. For this, we first prepared the Pfs–chitosan conjugate solution by incubating chitosan (buffered to pH 6.0 by the addition of sodium phosphate buffer), tyrosinase, and the pro-tagged Pfs (Fig. 1(b)). Tyrosinase activates the pro-tag to covalently conjugate Pfs to the chitosan in solution. Next, we electrodeposited Pfs–chitosan conjugate onto the patterned assembly site inside a microfluidic channel by filling the microchannel with Pfs–chitosan conjugate solution and then applying negatively biased electrical signals to the patterned elec-

trode (Fig. 1(c)). This microchannel was previously incubated in BSA solution to block non-specific binding of Pfs to the channel surfaces. Next, we continually transported through the microchannel a solution containing the substrate SAH, which was catalytically converted into reaction products SRH and adenine by the assembled Pfs (Fig. 1(d)). Finally, we performed HPLC analysis of the enzymatic reaction mixtures collected downstream.

As shown in Fig. 3(a), Pfs–chitosan conjugate was first assembled onto the assembly site in the microchannel by applying negatively-biased electrical signals (day 1), and enzymatic reactions were performed by continuously pumping SAH solution through the channel in a cyclic manner between $3 \mu\text{L min}^{-1}$ and $22 \mu\text{L min}^{-1}$, as shown in Fig. 3(b) (day 2). Reaction mixtures collected downstream were analyzed by HPLC. Next, Pfs enzyme was disassembled by mild acid solution (day 2), SAH was continuously pumped through the channel (day 3), and HPLC analysis was performed on the solutions collected downstream to demonstrate that Pfs enzyme was in fact completely disassembled and the device was cleaned for reuse. With the acid wash completed, Pfs–chitosan conjugate from the same solution batch was re-assembled (day 3), and enzymatic reactions were performed at the same flow rates, as shown in Fig. 3(b) (day 4), to demonstrate reproducible enzyme assembly and catalytic activity. Finally, the assembled enzyme was left in PBS buffer for 4 days at room temperature (days 4–7) before the final cycle of enzymatic reactions were performed (day 8) to demonstrate the stability of the assembled enzyme with extended time.

The HPLC analysis results in Fig. 3(c) show the following behavior. (1) By varying the flow rate in a cyclic manner between $3 \mu\text{L min}^{-1}$ (low flow rate) and $22 \mu\text{L min}^{-1}$ (high flow rate), the SAH conversion correspondingly cycled between $46 \pm 4\%$ at the low flow rate and $12 \pm 1\%$ at the high flow rate (day 2). (2) After cleaning the channel with mild acid solution, there is no conversion (day 3), demonstrating that the assembled enzyme was in fact completely removed, and thus allowing for repeated biofunctionalization and reuse of the bioMEMS device. (3) After re-assembly of Pfs enzyme, the SAH conversion recovered back to the cyclic behavior, alternating between $46 \pm 4\%$ and $12 \pm 1\%$ (day 4), demonstrating reproducible enzyme assembly and catalytic activity. (4) After leaving the enzyme in the microfluidic environment at room temperature for 4 days (days 4–7), the conversion cycled between $33 \pm 2\%$ and 9% (day 8). Specifically, the $33 \pm 2\%$ conversion represents $>70\%$ of the original conversion ($46 \pm 4\%$), demonstrating the stability of the enzyme with extended time. These results show that our model enzyme Pfs was successfully and robustly assembled onto readily addressable sites within prefabricated and packaged microfluidic channels by one-step electrodeposition of the Pfs–chitosan conjugate. Importantly, the assembled enzyme retained reproducible activity throughout the repeated flow cycles.

Combined, these results demonstrate the reproducibility of enzyme catalytic activity, the spatial and temporal programmability of our enzyme assembly process, the robustness and stability of the assembled enzyme with time, and the reusability of the devices when using our electrochemical enzyme assembly process.

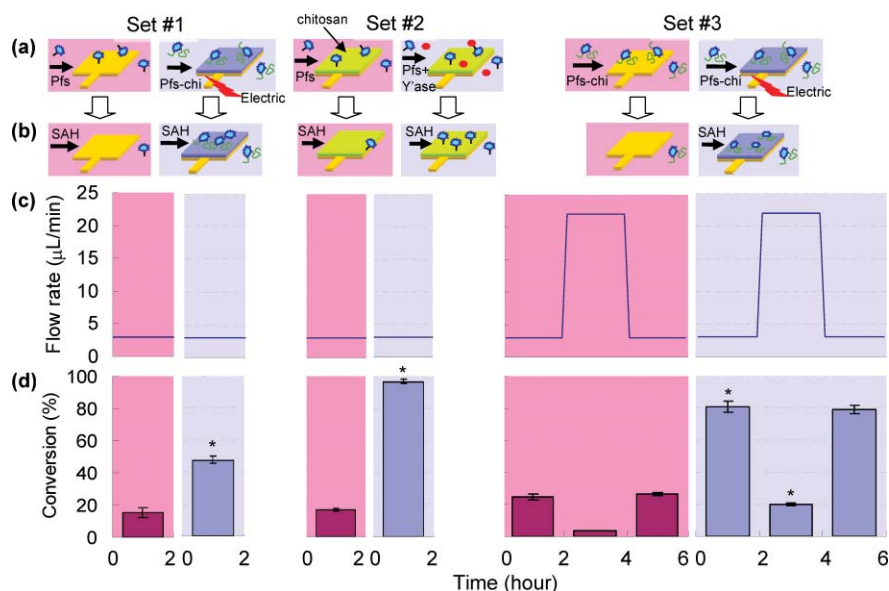


Fig. 4 Negative controls and corresponding experiments. Set #1 was designed to test the non-specific binding of free Pfs in bioMEMS without chitosan (or Pfs–chitosan conjugate) on the assembly electrode. Set #2 was designed to test the non-specific binding of free Pfs in bioMEMS with pre-deposited chitosan on the assembly electrode but without adding tyrosinase to *in situ* activate the pro-tag on Pfs molecules. Set #3 was designed to test the non-specific binding of Pfs–chitosan conjugate in bioMEMS without biasing the electrode, which was performed in a new microchannel and with a new batch of Pfs–chitosan conjugate solution. (a) Preparation of assembly site surface. Green = pure chitosan, blue = Pfs–chitosan conjugate. (b) Enzymatic reactions. (c) Flow rates. (d) Enzymatic conversions. All experiments show 3–6 times more conversion than the corresponding negative controls, despite the fact that the active electrode comprises only a small fraction (0.2%) of the total surface area available for non-specific binding within the bioMEMS. The * denotes a statistical difference ($p < 0.01$ in all cases).

each conjugate can be electrodeposited onto its own assembly site within a microchannel.

We believe the most stringent control was in experiment Set #3, which was designed to test the non-specific binding of Pfs–chitosan conjugate in bioMEMS without biasing the assembly electrode. This was performed in a new microchannel and with a new batch of Pfs–chitosan conjugate solution. Following the similar experimental procedure shown in Table 1, we first incubated the microchannel in BSA solution to block non-specific binding of Pfs to the channel surfaces. Next, we performed the experiment by electrodepositing Pfs–chitosan conjugate onto the patterned assembly site, and conducting enzymatic reactions by cycling the SAH flow rate between $3 \mu\text{L min}^{-1}$ and $22 \mu\text{L min}^{-1}$ and analyzed the reaction products *via* HPLC. Following the same procedure, the negative control was performed in the same microchannel after rinsing with acid solution, except that no electrical signal was applied during Pfs–chitosan conjugate incubation. The HPLC analysis of the enzymatic reaction products in Fig. 4(d) shows that at $3 \mu\text{L min}^{-1}$ flow rate, there was $25 \pm 3\%$ conversion of SAH into SRH and adenine in the negative control, while there was $79 \pm 4\%$ conversion in the experiment. At $22 \mu\text{L min}^{-1}$ flow rate, there was $3 \pm 1\%$ conversion in the negative control and $19 \pm 1\%$ conversion in the experiment. The conversion difference at $3 \mu\text{L min}^{-1}$ flow rate in experiment Set #1 ($48 \pm 2\%$) *versus* Set #3 ($79 \pm 4\%$) might be because the experiment Set #3 was performed within a different microchannel and with a new batch of Pfs–chitosan conjugate solution.

Performance of enzyme assembled on electrode

In all three experimental sets shown in Fig. 4, the results consistently yield 3–6 times more conversion than the corresponding negative controls, which demonstrates that the majority of conversion resulted from catalytic reactions at the target electrode sites. We confirmed that there was a significant statistical difference between the enzymatic conversion of the negative control and that of the experiment in each set by analyzing *via* single-factor ANOVA tests and multiple comparison tests ($p < 0.01$). For Set #3, this analysis was performed on conversions at both 3 and $22 \mu\text{L min}^{-1}$ flow rates. This is particularly striking because (1) the electrode site comprises only 0.2% of the total surface area within the bioMEMS device available for non-specific binding of the enzyme, and (2) the fluid volume above the electrode site comprises only 0.3% of the total fluid volume in the bioMEMS available for trapping free, unattached, solution-phase enzyme. In other words, these results demonstrated that the enzyme intentionally assembled on the electrode is far more ($>10^3 = 3\text{--}6/0.2\%$) efficient than the enzyme at non-specific binding sites in the entire microchannel.

We are currently optimizing our bioMEMS design to further minimize system dead volume, and are investigating alternative methods for blocking non-specific enzyme attachment. Nonetheless, non-specific protein attachment and system dead volume are issues common in biofunctionalized bioMEMS systems, due to the structural characteristics of enzymes and other proteins, the high surface area to volume ratio of the

system, and the minimal mixing due to the laminar flow characteristics of the system.^{1,13,21,44}

Enzyme stability and activity

The experimental results in Fig. 3(c) show that the assembled enzyme on the selected site in the microfluidic channel retained substantial catalytic activity for at least four days. We further examined Pfs stability by comparing specific catalytic activities over 4 days of the surface-assembled Pfs–chitosan conjugate at the electrode in a microchannel to (1) unassembled Pfs–chitosan conjugate solution and to (2) free and unconjugated Pfs solution (Table 2). For this, we reacted the Pfs solutions (1) and (2) with SAH on day 1 and then re-reacted the same Pfs solutions with fresh SAH on day 5. The free Pfs–chitosan conjugate formed a suspension when it was mixed with SAH substrate (due to the higher pH of SAH solution). All reaction mixtures were analyzed *via* HPLC. Shown in Table 2 are the specific activities of the experiments on day 1 and on day 5 after remaining 4 days at room temperature in PBS buffer, calculated as $\mu\text{mol SAH converted per min per mg Pfs}$ ($\mu\text{mol SAH min}^{-1} \text{ mg Pfs}^{-1}$). For the case of the unassembled conjugate, we assumed that all of the initially available Pfs had conjugated to chitosan during the conjugation reaction (as chitosan was added in excess of Pfs). For the case of the assembled conjugate, the mg Pfs assembled was estimated by electrodepositing Pfs–chitosan conjugate onto a microfabricated chip under the same conditions, and then resolubilizing the conjugate with dilute hydrochloric acid and performing Western blot analysis. Further information can be found in the electronic supplementary information.†

Table 2 shows that on the first day the specific activity of the assembled Pfs–chitosan conjugate is $1.8 \mu\text{mol SAH min}^{-1} \text{ mg Pfs}^{-1}$, while the specific activities of the unassembled conjugate suspension and the free unconjugated Pfs solution are $12 \mu\text{mol SAH min}^{-1} \text{ mg Pfs}^{-1}$: both values are within the range of reported Pfs specific activities, which vary over 3 orders of magnitude.^{32,45,46} The decrease in activity upon assembly is not surprising, given the steric hindrance effects of immobilized enzymes, and the diffusional limitations due to the minimal mixing associated with laminar flow in bioMEMS systems.

However, Table 2 demonstrates that the activity of the assembled Pfs–chitosan conjugate is better retained with time, as shown by the % activities remaining after 4 days incubation in PBS buffer at room temperature: 70% remaining for the

assembled conjugate, only 26% remaining for the conjugate suspension, and only 13% remaining for the free unconjugated enzyme. We conclude that the assembled enzymes in our bioMEMS are more stable and resistant to environmental changes for better retention of catalytic activities with time than are the bulk free or chitosan-conjugated enzyme solutions; thus, our approach allows for repeated use of the bioMEMS in continuous or intermittent processes. This stability advantage for surface-assembled enzyme over those in bulk solution is consistent to what has been observed in literature.⁴⁷

Transient response

Using our current bioMEMS packaging system, we observed a time delay between changing the flow rate over the reaction site (assembled with Pfs enzyme) and measuring the corresponding change in SAH concentration at the sample collection point downstream. To further understand the transient system response, we performed numerical modeling of the bioMEMS by simulating the mixing purely due to mass diffusion and laminar transport (Reynolds number = 0.1). The simulation result in Fig. 5 shows that in the low flow rate case ($3 \mu\text{L min}^{-1}$) it takes 10 min for a concentration change at the reaction site to travel downstream and arrive at the sample collection site, and it takes 25 min for the concentration response at the sample collection site to reach 95% of the concentration change at the reaction site. This is mainly due to dead volume ($\sim 20 \mu\text{L}$) in the packaging between the microchannel and the external

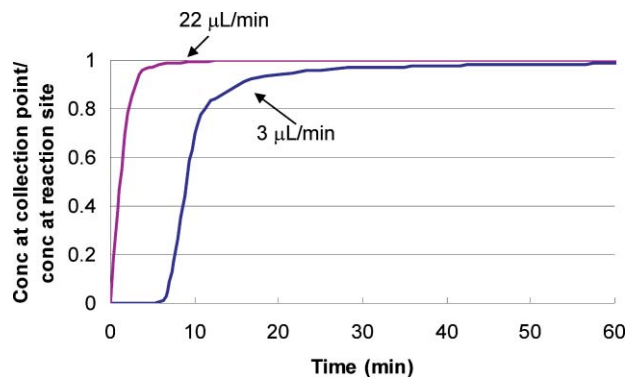


Fig. 5 Simulation of the transient concentration response at sample collection point to the concentration change at reaction site. (a) At $3 \mu\text{L min}^{-1}$ flow rate (blue). (b) At $22 \mu\text{L min}^{-1}$ flow rate (purple).

Table 2 Estimated specific catalytic activities of assembled Pfs–chitosan conjugate in microchannel, Pfs–chitosan conjugate suspension, and free unconjugated Pfs enzyme solution on day 1 and on day 5 after 4 days in PBS buffer at room temperature

Enzyme conditions	Specific activity day 1/ $\mu\text{mol SAH min}^{-1} \text{ mg Pfs}^{-1}$	Specific activity day 5/ $\mu\text{mol SAH min}^{-1} \text{ mg Pfs}^{-1}$	% activity after 4 days
<i>Heterogenous</i> : Assembled Pfs–chitosan conjugate in bioMEMS	3.7 ^a	2.6 ^a	70.4
<i>Homogenous</i> : Unassembled enzyme Pfs–chitosan conjugate ^b in batch reactors	12.1	3.2	26.4
Unconjugate free Pfs	12.0	1.5	12.8

^a The enzymatic reaction by the assembled Pfs–chitosan conjugate on spatially selected sites in a bioMEMS channel is heterogeneous. Quantification of the specific activities is more difficult than that in homogeneous reactions and is the focus of ongoing research. Assumptions were made to estimate the specific activities shown in the table, and more details are available in the ESI.† ^b Free Pfs–chitosan conjugate forms a suspension when it was mixed with SAH due to the higher pH of SAH solution.

tubing. This transient response of the bioMEMS justifies that we collected the samples for HPLC analysis only at the 2nd hour in each flow rate step after the concentration completely stabilized. The response time of the current system design also partially explains the conversions in the control experiment as any enzyme in the dead volume contributes to the enzymatic conversion. The minimization or elimination of dead volume is also under investigation and will be a focus of subsequent studies.

Discussion

Background

Recently the aminopolysaccharide chitosan,^{43,48–54} a key enabling material for biofabrication,⁵⁵ has been intensively exploited for post-fabrication biofunctionalization on patterned inorganic surfaces. Briefly, chitosan's pH responsive properties enable electrical signal-guided assembly of chitosan onto user-selected conductive inorganic surfaces from aqueous solution, and chitosan's abundant primary amine groups enable covalent conjugation of biomolecules to chitosan. We have demonstrated *in situ* protein assembly onto a chitosan scaffold in a bioMEMS device by chemically activating the amine groups of chitosan with glutaraldehyde.⁴³ We have also demonstrated *in situ* biochemical activation and protein assembly onto a chitosan scaffold in a microfluidic device.⁵⁶ In both reports, the assembled model protein green fluorescence protein (GFP) retained fluorescence and hence its 3-dimensional structure. Additionally, we reported that GFP preferentially assembles onto a chitosan scaffold through the C-terminal pentatyrosine pro-tag upon biochemical activation, demonstrating orientational control of protein assembly.⁵⁷

Enzyme assembly and activity in bioMEMS

Here we report an enzyme assembly strategy and demonstrate corresponding enzymatic activity based on electrodeposition of the enzyme-chitosan conjugate onto readily addressable electrode sites into a microchannel of a pre-fabricated and packaged bioMEMS device. Specifically, we report assembly of Pfs enzyme, a member of the AI-2 biosynthesis pathway, which catalyzes the cleavage of SAH into SRH and adenine. The significance of this result is that enzymes can be programmably assembled within a bioMEMS, while maintaining their catalytic activity over time. This provides the underpinnings for a viable bioMEMS technology platform to support metabolic engineering research and development for applications from elucidating biochemical reaction kinetics to discovering new drugs.

Our enzyme assembly strategy described here offers several unique advantages over conventional techniques, such as microcontact printing¹⁹ and self assembly layers.¹⁶ First, the enzymes conjugated to chitosan are covalently bonded, and the assembly of the enzyme-chitosan conjugate onto the patterned electrode in the microchannel can be programmed conveniently by electrical signals. Second, the enzyme assembly is performed in mild aqueous conditions inside prefabricated and completely packaged bioMEMS devices, thus avoiding direct contact and complex facilities. Third, we achieve temporal programmability, since we are able to assemble the enzymes just prior to using the enzyme for small molecule biocatalysis. This is advantageous for biological components that have limited shelf life.

Quantification

While the purpose of this paper was to demonstrate the assembly and activity of enzymes within the bioMEMS, quantification of the activity and comparison to alternatives is an important and natural question. Such quantification is challenging and is the subject of ongoing research. In the meantime, it is possible here to identify or estimate several semi-quantitative results of note.

Fig. 4(d) shows that some parasitic or background reaction occurs, presumably through non-specific enzyme assembly onto the microchannel surfaces^{13–25} or through any free, unattached, solution-phase enzyme. Fig. 4(d) also demonstrates that such conversion is significantly less and statistically different compared to the conversion achieved by the electrodeposited enzyme-chitosan conjugate. Additionally, the electrode, with only 0.5 mm² area, represents only 0.2% of the total microenvironment surface (221 mm²), and the volume above the electrode site (0.075 μL) represents only 0.3% of the total microenvironment volume (23.9 μL). Therefore, the enzyme-activated electrode is >3 orders of magnitude more efficient in executing the catalytic reaction than other areas of the microfluidic environment.

In a meaningful sense, these quantitative results are already encouraging. An overriding concern with microfluidics technology and applications is that the vastly enhanced surface : volume ratio *cf.* conventional chemical reactors may dramatically alter pathways and kinetics, rendering microfluidic environments not viable. For localized reaction sites in a bioMEMS, the concern takes two somewhat different but equally important forms: (1) will nonspecific binding at the large area of channel surface dominate over the small area of an active electrode? And (2), will parasitic reaction of enzyme in the aqueous phase of the entire channel volume dominate over that at the electrode? Results here show that the assembled enzyme on the small electrode *can* control the catalytic conversion of small molecules in the bioMEMS.

Optimization

There is ample opportunity to optimize conversion rates in our bioMEMS environments.⁵⁶ One means is through process parameters, such as flow rates, process time, concentrations, surface passivation, and pH. Another is through device design, such as channel dimensions and geometry, reduction of dead volumes, such as reservoirs, and new network designs which minimize cross-talk between enzyme assembly and subsequent catalytic conversion. With present conversion rates of 46%, there is room to improve the efficiency of enzyme conversion at the electrode, and reduction of parasitic conversion pathways (non-specific binding at channel surfaces and/or reaction in aqueous volumes), control and specificity of reaction at the active electrode sites can be improved as well.

Conclusions

This work demonstrates a chitosan-mediated biofunctionalization strategy for the assembly of catalytically active enzymes onto spatially and temporally programmed sites within a completely packaged and systematically controlled bioMEMS device. The HPLC analysis of downstream reaction mixtures

demonstrates that the assembled enzymes are catalytically active, robust, and stable with time, and that our strategy is reproducible, allowing for multiple uses of bioMEMS devices. While further quantification is needed, the assembled enzyme at the small active electrode is much more effective overall in catalytic conversion of the SAH substrate than are parasitic channels associated with non-specific enzyme attachment to the channel surfaces or with solution-phase enzyme. In any case, we report here for the first time the signal-guided assembly of catalytically active enzymes at localized sites, which can be programmed both spatially and temporally within a pre-packaged bioMEMS. The demonstration of their catalytic activity represents a key step in progress toward a bioMEMS technology to support metabolic engineering research and development, where multi-step biochemical reactions are common and separation of these steps is highly desirable for understanding reaction details and modifying pathways and kinetics for various applications (e.g. drug discovery).

This novel strategy of enzyme assembly was achieved through two unique techniques: (1) the covalent conjugation of the enzyme to chitosan in solution upon biochemical activation of a pro-tag and (2) the electrodeposition of the resulting enzyme–chitosan conjugate. Because the assembly of biological elements is signal-guided through the electrodeposition process, the active biology (enzyme–chitosan conjugate) can be introduced into prefabrication bioMEMS devices upon demand. We anticipate that the methodology can be extended to multiple sites and with different enzymes to accommodate multi-step metabolic pathways,⁵⁸ as would be valuable for replicating specific bacterial pathways and seeking new antimicrobial drugs that modify or suppress those pathways.

Acknowledgements

This work was supported in part by the Robert W. Deutsch Foundation, the NSF IMI program under DMR0231291, the USDA, the Laboratory for Physical Sciences and the Maryland NanoCenter.

References

- 1 D. J. Beebe, G. A. Mensing and G. M. Walker, *Annu. Rev. Biomed. Eng.*, 2002, **4**, 261–286.
- 2 J. W. Hong, Y. Chen, W. F. Anderson and S. R. Quake, *J. Phys.: Condens. Matter*, 2006, **18**, S691–S701.
- 3 J. Atencia and D. J. Beebe, *Nature*, 2005, **437**, 648–655.
- 4 T. Vilknær, D. Janasek and A. Manz, *Anal. Chem.*, 2004, **76**, 3373–3385.
- 5 P. S. Dittrich, K. Tachikawa and A. Manz, *Anal. Chem.*, 2006, **78**, 3887–3907.
- 6 D. Psaltis, S. R. Quake and C. H. Yang, *Nature*, 2006, **442**, 381–386.
- 7 H. Andersson and A. Van Den Berg, *Sens. Actuators, B*, 2003, **92**, 315–325.
- 8 D. R. Reyes, D. Iossifidis, P. A. Aurox and A. Manz, *Anal. Chem.*, 2002, **74**, 2623–2636.
- 9 P. A. Aurox, D. Iossifidis, D. R. Reyes and A. Manz, *Anal. Chem.*, 2002, **74**, 2637–2652.
- 10 H. Andersson and A. Van Den Berg, *Lab Chip*, 2006, **6**, 467–470.
- 11 U. Bilitewski, M. Genrich, S. Kadow and G. Mersal, *Anal. Bioanal. Chem.*, 2003, **377**, 556–569.
- 12 J. Shim, T. F. Bersano-Begoy, X. Y. Zhu, A. H. Tkaczyk, J. J. Linderman and S. Takayama, *Curr. Top. Med. Chem.*, 2003, **3**, 687–703.
- 13 B. S. Ku, J. H. Cha, A. Srinivasan, S. J. Kwon, J. C. Jeong, D. H. Sherman and J. S. Dordick, *Biotechnol. Prog.*, 2006, **22**, 1102–1107.
- 14 E. L'Hostis, P. E. Michel, G. C. Fiaccabrino, D. J. Strike, N. F. de Rooij and M. Koudelka-Hep, *Sens. Actuators, B*, 2000, **64**, 156–162.
- 15 P. L. Urban, D. M. Goodall and N. C. Bruce, *Biotechnol. Adv.*, 2006, **24**, 42–57.
- 16 N. K. Chaki and K. Vijayamohan, *Biosens. Bioelectron.*, 2002, **17**, 1–12.
- 17 C. S. Lee, S. H. Lee, Y. G. Kim, C. H. Choi, Y. K. Kim and B. G. Kim, *Biotechnol. Bioprocess Eng.*, 2006, **11**, 146–153.
- 18 D. Kisailus, Q. Truong, Y. Amemiya, J. C. Weaver and D. E. Morse, *Proc. Natl. Acad. Sci. U. S. A.*, 2006, **103**, 5652–5657.
- 19 A. P. Quist, E. Pavlovic and S. Oscarsson, *Anal. Bioanal. Chem.*, 2005, **381**, 591–600.
- 20 Y. Liu, W. Zhong, S. Meng, J. L. Kong, H. J. Lu, P. Y. Yang, H. H. Girault and B. H. Liu, *Chem.-Eur. J.*, 2006, **12**, 6585–6591.
- 21 H. B. Mao, T. L. Yang and P. S. Cremer, *Anal. Chem.*, 2002, **74**, 379–385.
- 22 C. M. Niemeyer, R. Wacker and M. Adler, *Nucleic Acids Res.*, 2003, **31**.
- 23 C. A. Malpass, K. W. Millsap, H. Sidhu and L. B. Gower, *J. Biomed. Mater. Res.*, 2002, **63**, 822–829.
- 24 Y. G. Li, Y. X. Zhou, J. L. Feng, Z. H. Jiang and L. R. Ma, *Anal. Chim. Acta*, 1999, **382**, 277–282.
- 25 J. L. Deng, C. X. Guo, W. S. Lu, T. Liu and L. Jiang, *Prog. Chem.*, 2006, **18**, 1397–1408.
- 26 D. C. Duffy, J. C. McDonald, O. J. A. Schueller and G. M. Whitesides, *Anal. Chem.*, 1998, **70**, 4974–4984.
- 27 B. H. Jo, L. M. Van Lerberghe, K. M. Motsegood and D. J. Beebe, *J. Microelectromech. Syst.*, 2000, **9**, 76–81.
- 28 J. C. McDonald, D. C. Duffy, J. R. Anderson, D. T. Chiu, H. K. Wu, O. J. A. Schueller and G. M. Whitesides, *Electrophoresis*, 2000, **21**, 27–40.
- 29 W. J. Chang, D. Akin, M. Sedlak, M. R. Ladisch and R. Bashir, *Biomed. Microdev.*, 2003, **5**, 281–290.
- 30 G. C. Randall and P. S. Doyle, *Proc. Natl. Acad. Sci. U. S. A.*, 2005, **102**, 10813–10818.
- 31 M. A. Unger, H. P. Chou, T. Thorsen, A. Scherer and S. R. Quake, *Science*, 2000, **288**, 113–116.
- 32 J. A. Duerre, *J. Biol. Chem.*, 1962, **237**, 3737–3741.
- 33 M. J. Federle and B. L. Bassler, *J. Clin. Invest.*, 2003, **112**, 1291–1299.
- 34 V. Sperandio, A. G. Torres and J. B. Kaper, *Mol. Microbiol.*, 2002, **43**, 809–821.
- 35 V. Sperandio, A. G. Torres, J. A. Giron and J. B. Kaper, *J. Bacteriol.*, 2001, **183**, 5187–5197.
- 36 A. F. G. Barrios, R. J. Zuo, Y. Hashimoto, L. Yang, W. E. Bentley and T. K. Wood, *J. Bacteriol.*, 2006, **188**, 305–316.
- 37 J. Zhu, M. B. Miller, R. E. Vance, M. Dziejman, B. L. Bassler and J. J. Mekalanos, *Proc. Natl. Acad. Sci. U. S. A.*, 2002, **99**, 3129–3134.
- 38 D. Balestrino, J. A. J. Haagensen, C. Rich and C. Forestier, *J. Bacteriol.*, 2005, **187**, 2870–2880.
- 39 D. C. Ren, J. J. Sims and T. K. Wood, *Environ. Microbiol.*, 2001, **3**, 731–736.
- 40 T. B. Rasmussen, M. E. Skindersoe, T. Bjarnsholt, R. K. Phipps, K. B. Christensen, P. O. Jensen, J. B. Andersen, B. Koch, T. O. Larsen, M. Hentzer, L. Eberl, N. Hoiby and M. Givskov, *Microbiology*, 2005, **151**, 1325–1340.
- 41 T. B. Rasmussen, T. Bjarnsholt, M. E. Skindersoe, M. Hentzer, P. Kristoffersen, M. Kote, J. Nielsen, L. Eberl and M. Givskov, *J. Bacteriol.*, 2005, **187**, 1799–1814.
- 42 R. Fernandes, C. Y. Tsao, Y. Hashimoto, L. Wang, T. K. Wood, G. F. Payne and W. E. Bentley, *Metab. Eng.*, 2007, **9**, 228–239.
- 43 J. J. Park, X. L. Luo, H. M. Yi, T. M. Valentine, G. F. Payne, W. E. Bentley, R. Ghodssi and G. W. Rubloff, *Lab Chip*, 2006, **6**, 1315–1321.
- 44 M. A. Holden, S. Y. Jung and P. S. Cremer, *Anal. Chem.*, 2004, **76**, 1838–1843.
- 45 A. J. Ferro, A. Barrett and S. K. Shapiro, *Biochim. Biophys. Acta*, 1976, **438**, 487–494.
- 46 E. D. Ragione, M. Porcelli, M. Cartenifarina and V. Zappia, *Biochem. J.*, 1985, **232**, 335–341.
- 47 L. Q. Cao, *Curr. Opin. Chem. Biol.*, 2005, **9**, 217–226.
- 48 L. Q. Wu, A. P. Gadre, H. M. Yi, M. J. Kastantin, G. W. Rubloff, W. E. Bentley, G. F. Payne and R. Ghodssi, *Langmuir*, 2002, **18**, 8620–8625.

- 49 L. Q. Wu, H. M. Yi, S. Li, G. W. Rubloff, W. E. Bentley, R. Ghodssi and G. F. Payne, *Langmuir*, 2003, **19**, 519–524.
- 50 H. M. Yi, S. Nisar, S. Y. Lee, M. A. Powers, W. E. Bentley, G. F. Payne, R. Ghodssi, G. W. Rubloff, M. T. Harris and J. N. Culver, *Nano Lett.*, 2005, **5**, 1931–1936.
- 51 H. M. Yi, L. Q. Wu, R. Ghodssi, G. W. Rubloff, G. F. Payne and W. E. Bentley, *Anal. Chem.*, 2004, **76**, 365–372.
- 52 H. M. Yi, L. Q. Wu, R. Ghodssi, G. W. Rubloff, G. F. Payne and W. E. Bentley, *Langmuir*, 2005, **21**, 2104–2107.
- 53 R. Fernandes, H. M. Yi, L. Q. Wu, G. W. Rubloff, R. Ghodssi, W. E. Bentley and G. F. Payne, *Langmuir*, 2004, **20**, 906–913.
- 54 S. T. Koev, M. A. Powers, H. Yi, L.-Q. Wu, W. E. Bentley, G. W. Rubloff, G. F. Payne and R. Ghodssi, *Lab Chip*, 2007, **7**, 103–111.
- 55 H. M. Yi, L. Q. Wu, W. E. Bentley, R. Ghodssi, G. W. Rubloff, J. N. Culver and G. F. Payne, *Biomacromolecules*, 2005, **6**, 2881–2894.
- 56 A. T. Lewandowski, H. M. Yi, X. L. Luo, G. F. Payne, R. Ghodssi, G. W. Rubloff and W. E. Bentley, *Biotechnol. Bioeng.*, 2008, **99**, 499–507.
- 57 A. T. Lewandowski, D. A. Small, T. H. Chen, G. F. Payne and W. E. Bentley, *Biotechnol. Bioeng.*, 2006, **93**, 1207–1215.
- 58 G. Y. Jung and G. Stephanopoulos, *Science*, 2004, **304**, 428–431.